

Structural characterization of three semi-rigid tetracarboxylate-containing transition-metal coordination polymers

Jing-Jing Huang, Jie-Hui Yu*, Ji-Qing Xu*

College of Chemistry, Jilin University, Jiefang Road 2519, Changchun, Jilin 130012, China

ARTICLE INFO

Article history:

Received 23 March 2016

Accepted 18 May 2016

Available online 31 May 2016

Keywords:

Semi-rigidity

Tetracarboxylate

Coordination polymers

Photoluminescence

Magnetic property

ABSTRACT

Under hydro(solvo)thermal conditions, the reactions between transition-metal salts and tetracarboxylic acid molecules, with the assistance of organic base molecules, created three new coordination polymers, namely $[H_2(bpp)]_2[Zn_2(sph)_2] \cdot H_2O$ ($sph = 4,4'$ -sulfonediphthalate, $bpp = 1,3$ -bis(piperidyl)propane) **1**, $[H_2(bpp)]_2[Ni_2(oph)_2(H_2O)_2] \cdot 2H_2O$ ($oph = 4,4'$ -oxydiphthalate) **2** and $[H_2(bpe)]_2[Ni(Hfph)_2(bpe)]$ ($bpe = 1,2$ -bis(pyridyl)ethylene; $fph = 4,4'$ -(hexafluoroisopropylidene)diphthalate) **3**. X-ray single-crystal diffraction analysis reveals that (i) in **1**, the diprotonated bpp molecule acts as a templating agent. The quadruple-bridged sph molecules propagate the tetrahedral Zn^{2+} ions into a 2-D layer network in **1**, where two types of circle loops are found; (ii) in **2**, the bpp molecule is also diprotonated. The triple-bridged oph molecules extend the octahedrally coordinated Ni^{2+} ions into a 2-D layer network, in which a carboxylate-bridged Ni^{2+} chain is observed; (iii) in **3**, the non-protonated bpe molecules link the Ni^{2+} ions into a 1-D linear chain. The diprotonated bpe molecule acts as the counterion, while the fph molecule serves as the chelating ligand, existing in the form of $Hfph^{3-}$; and (iv) the 2-D layers for **1** and **2** can both be simplified as a (4,4) net. The photoluminescence analysis reveals that **1** emits blue light with a maximum at 415 nm upon excitation at 355 nm. A magnetic property investigation indicates that anti-ferromagnetic interactions exist between the Ni^{2+} ions in **2**.

© 2016 Elsevier Ltd. All rights reserved.

1. Introduction

Over the past fifty years, metal-multicarboxylate coordination polymer (CP) chemistry achieved rapid development [1–5]. Metal-multicarboxylate CPs not only possess the rich structures [6–10], many interesting physical properties have also been investigated [11–20]. For example, (i) porous metal-multicarboxylate CPs can selectively adsorb gases, in particular H_2 (for energy storage) and CO_2 (for purification of the environment) [21–25]; (ii) $Zn^{2+}/Cd^{2+}/Ln^{3+}$ -multicarboxylate CPs can emit light. Based on this property, some metal-multicarboxylate CPs have been developed into molecular devises, such as chemosensors [26–30]; and (iii) since the carboxylate groups can link metal ions to form various clusters or chains, the metal-multicarboxylate CPs exhibit excellent magnetic properties [31–35]. In the construction of the metal-multicarboxylate network, the multicarboxylate molecule plays a key role. By varying the size, charge, configuration, rigidity/flexibility, substituent, carboxylate number and the carboxylate

location, the multicarboxylate molecule directly affects the resulting network formation.

Recently, a class of semi-rigid multicarboxylic acid molecules has attracted the attention of researchers [36,37,32,38–44]. They generally consist of several benzene ring moieties. Two neighboring benzene rings are connected by a non-metallic atom or a group. The so-called semi-rigidity means that the tetrahedron for the centric non-metallic atom can be slightly distorted, and the two adjacent benzene rings can appropriately rotate around the centric atom. In the past, we have employed several semi-rigid multicarboxylic acid molecules to construct some CPs [45–49]. In this article, the semi-rigid tetracarboxylic acid molecules H_4sph ($sph = 4,4'$ -sulfonediphthalate), H_4oph ($oph = 4,4'$ -oxydiphthalate) and H_4fph ($fph = 4,4'$ -(hexafluoroisopropylidene)diphthalate) were selected, and with the assistance of organic base molecules, three new transition-metal CPs, $[H_2(bpp)]_2[Zn_2(sph)_2] \cdot H_2O$ ($bpp = 1,3$ -bis(piperidyl)propane) **1**, $[H_2(bpp)]_2[Ni_2(oph)_2(H_2O)_2] \cdot 2H_2O$ **2** and $[H_2(bpe)]_2[Ni(Hfph)_2(bpe)]$ ($bpe = 1,2$ -bis(pyridyl)ethylene) **3**, were obtained under hydro(solvo)thermal conditions. Here we will report their structural characterization.

* Corresponding authors. Tel.: +86 431 88499132; fax: +86 431 85168624.

E-mail addresses: jhyu@jlu.edu.cn (J.-H. Yu), xjq@mail.jlu.edu.cn (J.-Q. Xu).

2. Experimental

2.1. Materials and physical measurements

All chemicals were of reagent grade quality, obtained from commercial sources without further purification. Elemental analysis (C, H and N) was performed on a Perkin–Elmer 2400LS II elemental analyzer. Infrared (IR) spectra were recorded on a Perkin Elmer Spectrum 1 spectrophotometer in the 4000–400 cm⁻¹ region using a powdered sample on a KBr plate. Powder X-ray diffraction (XRD) data were collected on a Rigaku/max-2550 diffractometer with Cu K α radiation ($\lambda = 1.5418 \text{ \AA}$). Thermogravimetric (TG) behavior was investigated on a Perkin–Elmer TGA-7 instrument with a heating rate of 10 °C min⁻¹ in air. Fluorescence spectra were obtained on a LS 55 fluorescence/phosphorescence spectrophotometer at room temperature.

2.2. Synthesis of the title compounds

2.2.1. Synthesis of **1**

Colorless columnar crystals of **1** were obtained from the simple solvothermal self-assembly of Zn(OAc)₂·2H₂O (0.2 mmol, 44 mg), 4,4'-sulfonephthalic dianhydride (0.1 mmol, 36 mg) and bpp (0.1 mmol, 21 mg) in a 10 mL H₂O and CH₃OH solution (volume ratio = 4:1; pH = 7 neutralized by triethylamine) at 140 °C for 3 days. Yield: ca. 20% based on Zn(II). Anal. Calc. for C₅₈H₇₀N₄O₂₁S₂·Zn₂ **1**: C, 51.40; H, 5.21; N, 4.14. Found: C, 50.73; H, 5.09; N, 4.12%. IR (cm⁻¹): 2949 m, 2846 m, 1627 s, 1573 s, 1471 m, 1482 w, 1388 s, 1316 s, 1160 m, 1077 m, 903 m, 840 s, 675 s, 622 s, 498 m (see Fig. S1).

2.2.2. Synthesis of **2**

Green columnar crystals of **2** were obtained from the simple hydrothermal self-assembly of Ni(NO₃)₂·6H₂O (0.2 mmol, 58 mg), 4,4'-oxydiphtalic anhydride (0.1 mmol, 44 mg) and bpp (0.1 mmol, 21 mg) in a 10 mL aqueous solution (pH = 7 neutralized by dilute NaOH) at 120 °C for 3 days. Yield: ca. 17% based on Ni(II). Anal. Calc. for C₅₈H₇₆N₄Ni₂O₂₂ **2**: C, 53.64; H, 5.90; N, 4.31. Found: C, 54.03; H, 5.88; N, 4.30%. IR (cm⁻¹): 2933 w, 2852 w, 1584 s, 1559 s, 1398 s, 1253 m, 1222 m, 1155 w, 963 m, 918 w, 886 w, 961 w, 821 s, 622 w, 565 w, 520 w (see Fig. S1).

2.2.3. Synthesis of **3**

Green columnar crystals of **3** were obtained from the simple hydrothermal self-assembly of Ni(NO₃)₂·6H₂O (0.2 mmol, 58 mg), 4,4'-hexafluoroisopropylidene)diphthalic anhydride (0.1 mmol, 44 mg) and bpe (0.15 mmol, 27 mg) in a 10 mL aqueous solution (pH = 5 adjusted by dilute NaOH) at 120 °C for 3 days. Yield: ca. 15% based on Ni(II). Anal. Calc. for C₇₄H₄₈F₁₂N₆NiO₁₆ **3**: C, 56.83; H, 3.09; N, 5.34. Found: C, 56.92; H, 2.83; N, 5.37%. IR (cm⁻¹): 1714 s, 1606 s, 1579 s, 1502 w, 1420 s, 1259 s, 1206 w, 1181 m, 1161 w, 1067 w, 963 m, 902 w, 835 s, 716 w, 612 w, 551 w (see Fig. S1).

2.3. X-ray crystallography

The data were collected with Mo K α radiation ($\lambda = 0.71073 \text{ \AA}$) on a Siemens SMART CCD diffractometer. With the SHELXTL program, all of the structures were solved using direct methods [50]. The non-hydrogen atoms were assigned anisotropic displacement parameters in the refinement, and the other hydrogen atoms were treated using a riding model. The H atoms on the water molecules in **1** and **2**, and on the O6 atom in **3** were not located. The H atoms on the bpp molecule in **1** and **2** were not located, either. The struc-

Table 1
Crystal data of the title compounds.

	1	2	3
Formula	C ₅₈ H ₆₂ N ₄ O ₂₁ S ₂ Zn ₂	C ₅₈ H ₇₆ N ₄ O ₂₂ Ni ₂	C ₇₄ H ₄₈ N ₆ O ₁₆ F ₁₂ Ni
<i>M</i>	1346.04	1298.65	1563.87
<i>T</i> (K)	293(2)	293(2)	293(2)
Crystal system	monoclinic	triclinic	triclinic
Space group	<i>P</i> 2 ₁	<i>P</i> 1	<i>P</i> 1
<i>a</i> (Å)	9.8817(6)	10.0855(5)	9.2544(13)
<i>b</i> (Å)	24.8194(14)	10.7409(5)	13.5680(17)
<i>c</i> (Å)	12.3018(8)	13.5815(8)	13.938(2)
α (°)	90	98.241(3)	78.982(9)
β (°)	97.504(4)	91.246(3)	89.070(10)
γ (°)	90	94.517(3)	79.747(9)
<i>V</i> (Å ³)	2991.3(3)	1450.72(13)	1690.1(4)
<i>Z</i>	2	1	1
<i>D</i> _c (g cm ⁻³)	1.494	1.486	1.536
μ (mm ⁻¹)	0.953	0.734	0.397
Reflections collected	16966	8226	9561
Unique reflections	9953	5091	5962
<i>R</i> _{int}	0.0336	0.0248	0.0368
Goodness-of-fit (GOF) on <i>F</i> ²	1.043	1.058	1.079
<i>R</i> ₁ , <i>I</i> > 2σ(<i>I</i>)	0.0349	0.0369	0.0982
<i>wR</i> ₂ , all data	0.0961	0.1071	0.2931

tures were then refined on *F*² using SHELXL-97 [50]. The crystal data of **1–3** are summarized in Table 1.

3. Results and discussion

3.1. Synthetic analysis

All of the compounds were obtained under hydro(solvo)thermal conditions. In the reactions, the pH level of the reactive system plays a crucial role: (i) it directly influences the crystal growth. The optimal pH conditions for the crystal growth is 7 for **1**, 7 for **2**, and 5 for **3**; (ii) it directly influences the deprotonation reaction of the tetracarboxylic acid molecule. At pH = 7, the tetracarboxylic acid molecule completely deprotonates, as observed in **1** and **2**, while at pH = 5, it only partly deprotonates, as observed in **3**; and (iii) it directly influences the protonation reaction of the organic base molecule. As found in **1–3**, the organic base molecule has a potential to be protonated at pH ≤ 7, but obviously, the bpp molecule is more easily protonated than the bpe molecule, because at pH = 7, the protonation reaction for the bpp molecule has occurred, while at pH = 5, the partial bpe molecule still exists in the form of the neutral molecule.

3.2. Structural description

3.2.1. Structural description of **1**

1 is a sph-bridged 2-D layered Zn²⁺ CP. Bpp should exist in the diprotonated form in order to balance the systematic charge. **1** crystallizes in the space group *P*2₁ and the asymmetric unit is found to be composed of two types of Zn²⁺ ions (Zn1 and Zn2), two types of sph molecules (sph I, sph II), two types of H₂(bpp)²⁺ molecule (bpp I, bpp II) and one lattice water molecule (Ow1). Since the two types of Zn²⁺ ions have the same coordination environment and the two types of sph molecules adopt the same coordination mode, only Zn1 and sph I, as representatives, are described. As shown in Fig. 1c, the Zn1 ion is in a tetrahedral site, completed by four carboxylate O atoms (O2, O8a, O10a, O12). The Zn1–O bond length range is 1.930(2)–2.007(2) Å. Fig. 1d shows the coordination environment around the Zn2 ion. The sph I ligand adopts the $\eta^1:\eta^0:\eta^1:\eta^1:\eta^1:\eta^0:\eta^1:\mu_3$ coordination mode (see

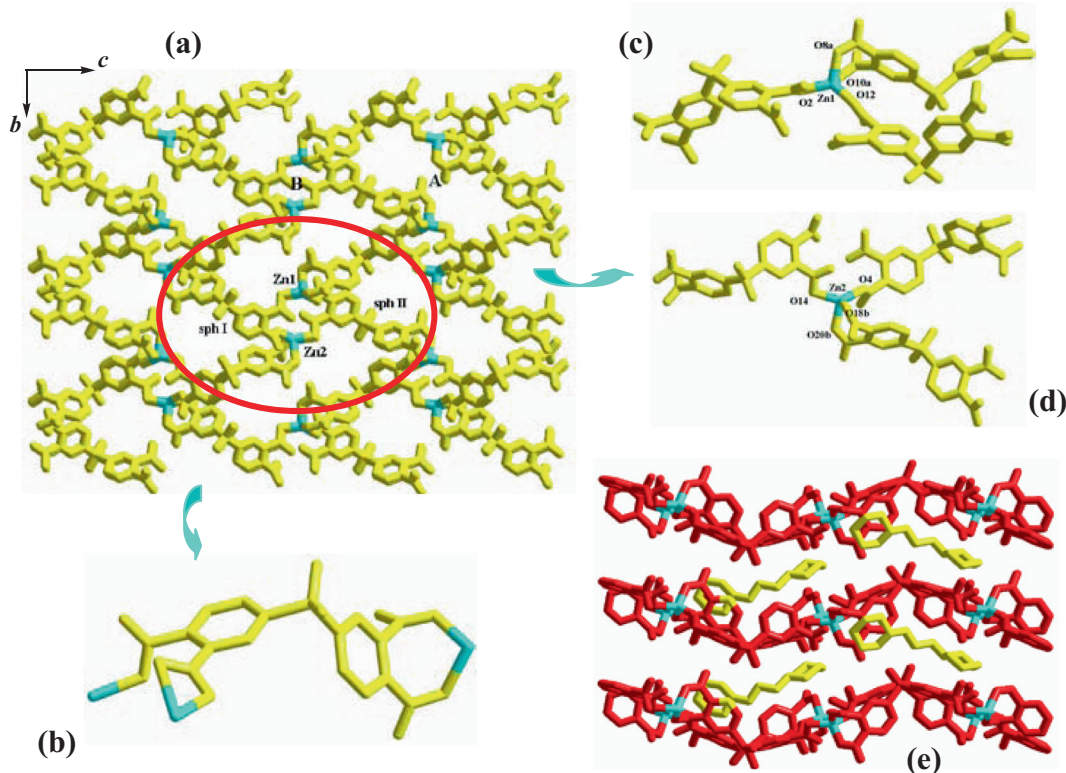


Fig. 1. 2-D layer network (a), coordination mode of sph (b), coordination environments around Zn1 (c) and Zn2 (d), and projection plot in the (001) direction (e) in **1** (a: $-x - 2, y + 1/2, -z - 2$; b: $-x - 3, y - 1/2, -z - 3$).

Fig. 1b). The triple-bridged sph molecules link the tetrahedral Zn^{2+} centers into a 2-D layer network in **1** (see Fig. 1a). In the layer, two types of circle loops (loops A and B) are observed. Loop A is comprised of four Zn^{2+} centers and four sph molecules, linked through an alternate arrangement, while an alternate arrangement of two Zn^{2+} centers and two phthalate moieties forms loop B. Based on the topological method, the loop B can be viewed as a 4-connected node, while the sph molecule serves as a linker. So the 2-D layer of **1** has a simple (4,4)-topology. The shortest $Zn \cdots Zn$ separation in the layer is $Zn1 \cdots Zn2 = 5.617 \text{ \AA}$. As displayed in Fig. 1e, the bpp molecule serves as a templating agent, occupying the space between the 2-D layers. The bpp II molecules act as bridges, extending the Zn-sph layers into a 3-D supramolecular network via N-H \cdots O interactions ($N3 \cdots O17c = 2.796 \text{ \AA}$, $N4 \cdots O10d = 2.841 \text{ \AA}$), while two N atoms from bpp I form hydrogen bonds to the carboxylate O atoms from an identical Zn-sph layer ($N1 \cdots O20e = 2.750 \text{ \AA}$, $N2 \cdots O13f = 2.738 \text{ \AA}$, as shown in Fig. S2).

3.2.2. Structural description of **2**

2 is an oph-propagated 2-D layered Ni^{2+} CP. Bpp exists in the diprotonated form in **2**. **2** crystallizes in the space group $P\bar{1}$ and the asymmetric unit is found to be composed of two types of Ni^{2+} ions ($Ni1, Ni2$; occupancy ratio: 0.5 for each), one oph molecule, one diprotonated bpp molecule, one coordinate water molecule ($Ow1$) and one lattice water molecule ($Ow2$). Templating by $H_2(bpp)^{2+}$, **2** exhibits a 2-D layer structure, as shown in Fig. 2a. Two crystallographically independent Ni^{2+} centers are both in octahedral sites (see Fig. 2b and c). $Ni1$ is coordinate by four carboxylate O atoms ($O1, O1a, O7b, O7c$) and two water molecules ($Ow1, Ow1a$), while $Ni2$ is surrounded by six carboxylate O atoms ($O3d, O3e, O6, O6f, O8, O8f$). The $Ni-O_{\text{carboxylate}}$ distances span a narrow range from 1.9978(17) to 2.0851(16) \AA . The $Ni-Ow$ dis-

tance of 2.1055(17) \AA is slightly longer. Oph adopts a tetra-bridged coordination mode (see Fig. 2d). Each carboxylate group coordinates with one O atom ($O1, O3, O6, O7$) to one Ni^{2+} ion. Meanwhile, the O8 atom also participates in the coordination, sharing one Ni^{2+} center ($Ni2$) with O6. The $\mu 4$ -mode oph molecules link two types of octahedral $Ni(\text{II})$ centers into a 2-D layer network in **2**. Interestingly, a carboxylate-bridged Ni^{2+} chain is observed within the layer, in which this carboxylate group adopts a syn-anti mode. Based on the topological viewpoint, the Ni^{2+} center can be regarded as a 4-connected node, and the oph molecules acts as linkers. So the 2-D layer of **2** also possess a simple (4,4) topology. The shortest $Ni \cdots Ni$ contact distance in the layer is $Ni1 \cdots Ni2b = 5.043 \text{ \AA}$. The $H_2(bpp)^{2+}$ molecules occupy the space between the 2-D layers (see Fig. 2e). Via N-H \cdots O interactions ($N1 \cdots O4 = 2.690 \text{ \AA}$, $N2 \cdots O5 g = 2.735 \text{ \AA}$), the H_2bpp^{2+} molecules propagate the 2-D Ni-oph layers into a 3-D supramolecular network (see Fig. S3).

3.2.3. Structural description of **3**

3 is a bpe-extended 1-D chained Ni^{2+} CP. It crystallizes in the space group $P\bar{1}$ and the asymmetric unit is found to be composed of a half Ni^{2+} ion ($Ni1$), one fph molecule and two types of bpe molecules (bpe I and bpe II). Note, only a half bpe II molecule appears in the asymmetric unit of **3**. Fig. 3a plots the 1-D chain structure of **3**. Unprecedentedly, the fph molecule does not act as a bridging liand. It just chelates to a Ni^{2+} center with two O donors ($O1, O3$; $Ni1-O1 = 2.111(5) \text{ \AA}$, $Ni1-O3 = 2.051(5) \text{ \AA}$). Bpe II acts as a bridge, linking the octahedral Ni^{2+} centers into a 1-D linear chain ($\angle Ni \cdots Ni \cdots Ni = 179^\circ$), running down the c -axial direction. The $Ni1-N3$ distance is 2.100(5) \AA . Although the O7 and O8 atoms do not interact with the Ni^{2+} centers, this carboxylate group should be deprotonated, which is confirmed by the two equivalent C-O distances ($C28-O7 = 1.216(11) \text{ \AA}$, $C28-O8 = 1.219(12) \text{ \AA}$). The $C27-O5$ distance (1.242(12) \AA) is obviously shorter than that of

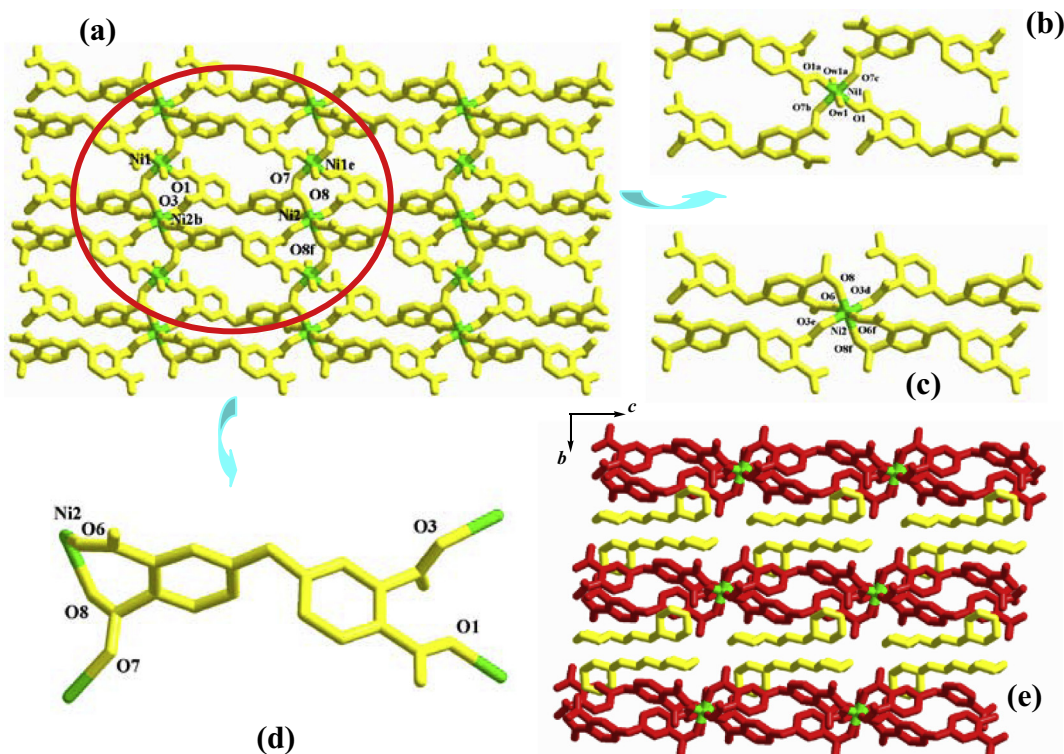


Fig. 2. 2-D layer network (a), coordination environments around Ni1 (b) and Ni2 (c), coordination mode of oph (d) and projection plot in the (100) direction (e) in **2** (a: $-x + 1$, $-y, -z + 2$; b: $x, y, z + 1$; c: $-x + 1, -y, -z + 1$; d: $-x, -y, -z + 1$; e: $x, y, z - 1$; f: $-x, -y, -z$).

C27–O6 ($1.295(14)$ Å), indicating that this carboxylate group does not deprotonate. So in **3**, fph has a -3 oxidation state and should be labeled as H(fph)^{3−}. The bpe I molecule should be diprotonated, in order to balance the system charge. As shown in Fig. 3b, both bpe I N atoms form hydrogen bonds to the adjacent carboxylate O atoms ($N1\cdots O2b = 2.546$ Å, $N2\cdots O7c = 2.701$ Å). Via the N–H···O interactions, the 1-D chains are propagated into a 2-D supramolecular sheet network. Since each Ni²⁺ center is surrounded by two fph molecules, the 2-D supramolecular sheet possesses a certain thickness. The octahedral Ni1 center is coordinated by four carboxylate O atoms (O1, O3, O1a, O3a) and two bpe N atoms (N3, N3a). No weak interactions are found between the 2-D supramolecular layers (see Fig. S4).

3.3. Structural discussion

In **1–3**, the tetracarboxylate molecules exhibit a semi-rigid character. On the one hand, the tetrahedral configurations for the centric non-metal atoms suffer from severe deformation: $106.55(16)$ – $120.0(2)$ ° in **1**, $117.5(2)$ ° in **2**, and $105.4(6)$ – $113.6(6)$ ° in **3**. On the other hand, the dihedral angle for the two benzene rings spans a wide range: 71.2 and 76.4 ° in **1**, 82.5 ° in **2**, and 76.5 ° in **3**. The semi-rigid character of the tetracarboxylate molecule is helpful for crystal growth. The bpp molecule is expected to serve as a linker in the compounds. However, in most reported compounds, it acts as a templating agent, similar to the situations observed in **1** and **2** [51–53]. Only in limited examples does the bpp molecule act as a linker, as found in the compound $[Cu_4I_4(bpp)_2]$ [54]. In the reported compounds $[H_2(bpp)][Mn_2(cpph)_2(H_2O)_2]$ (cpph = 4-(4-carboxyphenoxy)phthalate) [46] and $[H_2(bpp)][Mn_2(bcbob)_2]$ (bcbob = 3,5-Bis((4'-carboxylbenzyl)oxy)benzoilate) [48], the bpp molecule acts as a guest molecule. The formation of these two 3-D porous networks should be related to the

character of the molecules cpph and bcbob. While for the title tetracarboxylate molecules, it should be difficult to form a 3-D network with such large pores.

3.4. Characterization

3.4.1. TG analysis of **1–3**

The TG behaviors of **1–3** were investigated. Fig. 4 gives the temperature versus weight-loss curves. **1** underwent four steps of weight loss. Since the water content in **1** is rather low (Calcd: 1.34%), the first step of weight loss for **1** was not obvious (Found: ca. 1.50%). From ca. 310 °C, **1** underwent three-steps of continuous weigh loss, corresponding to the removal of the organic bpp and sph molecules. The final remaining residue was proven to be ZnO (Calcd: 12.09%; Found: ca. 13.23%). **2** underwent three steps of weight loss. The first step was a minor weight loss of ca. 4.50%, which should be attributed to sublimation of the water molecule in **2** (Calcd: 5.50%). From ca. 310 °C, the second step of weight loss for **2** started. In the temperature range of 310–455 °C, **2** underwent two-steps of continuous weigh loss, corresponding to the decomposition of the organic bpp and oph molecules. The final residue is NiO (Calcd: 11.50%; Found: ca. 11.50%). **3** was thermally stable up to ca. 270 °C. At about ca. 490 °C, the decomposition of the organic compositions in **3** completed; synchronously, Ni²⁺ combined with O₂ to generate NiO (Calcd: 4.78%; Found: ca. 4.89%).

3.4.2. Powder XRD patterns of **1–3**

Fig. 5 presents the experimental and simulated powder XRD patterns of **1–3**. The experimental powder XRD pattern for each compound is in accord with the simulated one generated on the basis of the structural data, confirming that the as-synthesized product is pure phase.

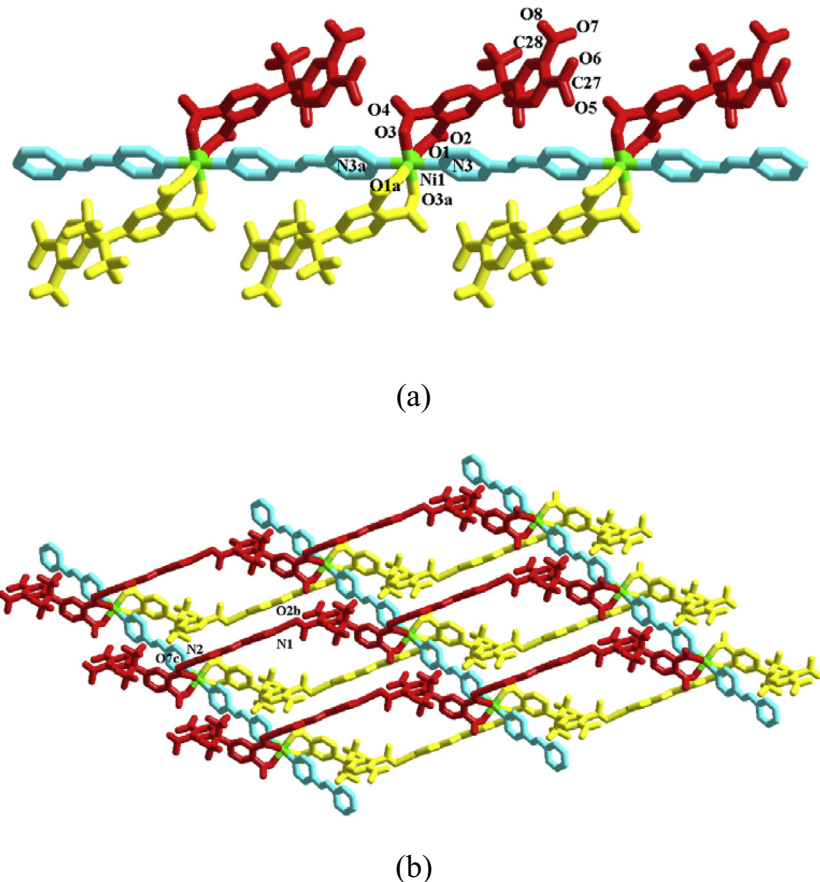


Fig. 3. 1-D chain (a) and 2-D supramolecular layer network (b) in **3** (a: $-x + 2, -y + 2, -z$; b: $x - 1, y - 1, z$; c: $x + 1, y, z$).

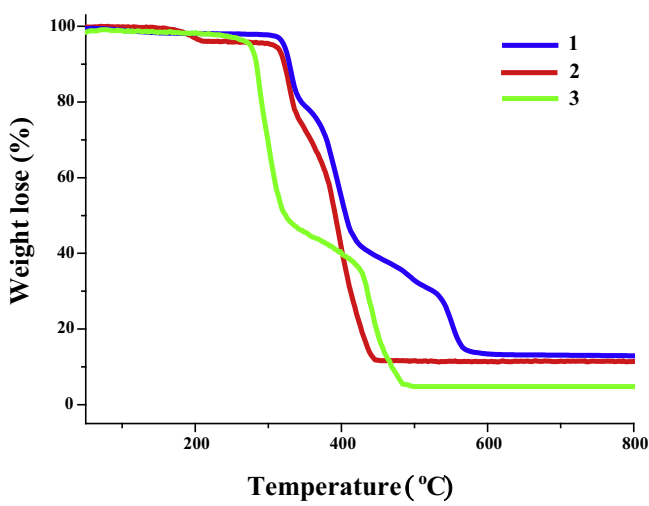


Fig. 4. TG curves of **1–3**.

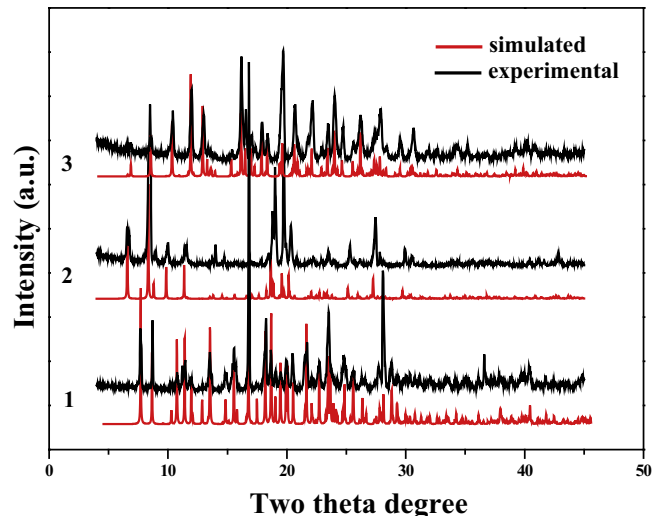


Fig. 5. Powder XRD patterns of **1–3**.

3.5. Properties

3.5.1. Photoluminescence property of **1**

The solid-state photoluminescence behavior of **1** at room temperature was investigated. As shown in Fig. 6 and **1** possesses photoluminescence, exhibiting a blue-light emission with a maximum at 415 nm when excited at 355 nm. Compared to the emission at

356 nm for free H₄sph ($\lambda_{\text{ex}} = 292$ nm) [55], the emission of **1** should also be assigned to a ligand-centered electronic excitation ($\pi^* \rightarrow \pi$), even though a larger red shift of 59 nm is observed. The red shift should be due to the coordination of sph to the metal center. For the other reported sph-containing complexes, a red-shift phenomenon is also observed [56–58].

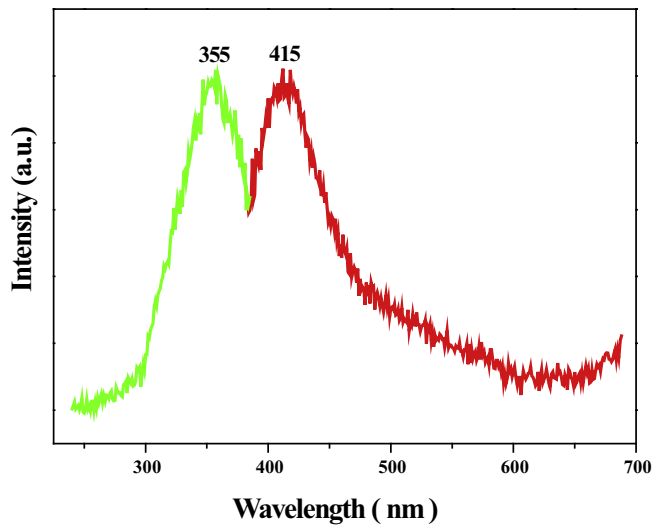


Fig. 6. Photoluminescence excitation (green) and emission (red) spectra of **1**. (Color online.)

3.5.2. Magnetic property of **2**

Magnetic susceptibility data were determined over the temperature of range 2–300 K at a magnetic field of 1000 Oe on a Quantum Design MPMS-7 SQUID magnetometer. The magnetic behavior of **2** is depicted in the form of χ_{MT} and χ_M^{-1} versus T plots (see Fig. 7). The experimental χ_{MT} product at 300 K is 1.723 emu K mol⁻¹, slightly lower than the theoretically expected value of 2 emu K mol⁻¹ for two non-interacting Ni²⁺ ions ($S = 1/2$, $g = 2.0$). Upon cooling down, the χ_{MT} value basically shows a decreasing trend within the whole temperature range, suggesting that antiferromagnetic interactions exist between the Ni²⁺ ions in **2**. Only in the narrow temperature range of 16–11 K, does the χ_{MT} product exhibit a slight increase from 0.397 to 0.411 emu K mol⁻¹. This should be unconnected to the spin-canting effect, because only a minor increase by 0.014 emu K mol⁻¹ is observed. The carboxylate-bridged Ni²⁺ chain in **2** should be responsible for its antiferromagnetic property, providing an effective path for magnetic exchange.

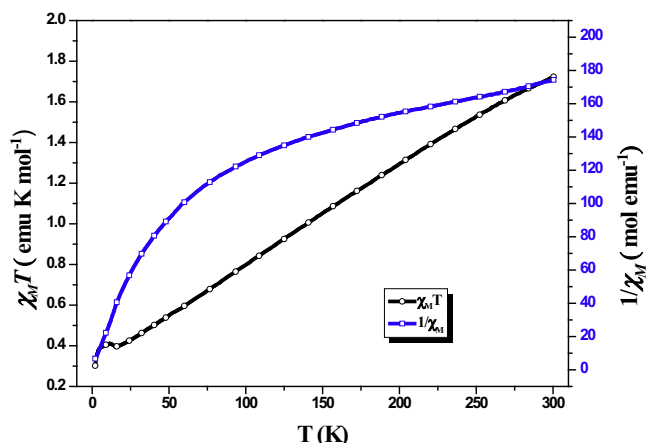


Fig. 7. Temperature dependence of χ_{MT} (black) and χ_M^{-1} (blue) vs. T for **2**. (Color online.)

4. Conclusion

In summary, we have reported the synthesis and structural characterization of three new semi-rigid tetracarboxylate-coordinated transition-metal CPs. Synthetically, the pH value of the reaction system plays a key role. It not only influences the crystal growth, but also influences the existing forms of the organic acid and base molecules. Structurally, the tetracarboxylate molecules in **1–3** exhibit a semi-rigid character in the formation of the network structures. The organic base molecule can assist the organic acid molecule to construct the new CP network. The bpp molecule tends to act as a counterion in the CP compounds. The spha-extended 2-D Zn²⁺ complex displays photoluminescence, whereas the oph-propagated 2-D Ni²⁺ complex shows antiferromagnetism.

Acknowledgements

This research was supported by the National Natural Science Foundation of China (No. 21271083).

Appendix A. Supplementary data

CCDC 1469986–1469988 contain the supplementary crystallographic data for **1–3** respectively. These data can be obtained free of charge via <http://www.ccdc.cam.ac.uk/conts/retrieving.html>, or from the Cambridge Crystallographic Data Centre, 12 Union Road, Cambridge CB2 1EZ, UK; fax: (+44) 1223-336-033; or e-mail: deposit@ccdc.cam.ac.uk. Supplementary data associated with this article can be found, in the online version, at <http://dx.doi.org/10.1016/j.poly.2016.05.054>.

References

- [1] L. Abutorabi, A. Morsali, *Coord. Chem. Rev.* 310 (2016) 116.
- [2] D. Bradshaw, S. El-Hankari, L. Lupica-Spagnolo, *Chem. Soc. Rev.* 43 (2014) 5431.
- [3] C. Pettinari, A. Tăbăcaru, S. Galli, *Coord. Chem. Rev.* 307 (2016) 1.
- [4] P.C. Silva, S.M.F. Vilela, J.O.P.C. Tome, F.A.A. Paz, *Chem. Soc. Rev.* 44 (2015) 6774.
- [5] P. Wei, X. Yan, F. Huang, *Chem. Soc. Rev.* 44 (2015) 815.
- [6] P.C. Cheng, Y.C. Lo, W. Hsu, K.B. Thapa, S.M. Liou, J.D. Chen, *Polyhedron* 96 (2015) 1.
- [7] Z. Xiao, X. Yang, S. Zhao, D. Wang, Y. Yang, L. Wang, *J. Solid State Chem.* 234 (2016) 36.
- [8] Q. Yue, Q. Huang, Y.Y. Gao, E.Q. Gao, *Inorg. Chim. Acta* 443 (2016) 110.
- [9] S. Zhang, Q. Yang, X. Liu, X. Qu, Q. Wei, G. Xie, S. Chen, S. Gao, *Coord. Chem. Rev.* 307 (2016) 292.
- [10] O. Hietsoi, A.S. Filatov, C. Dubceac, M.A. Petrukhina, *Coord. Chem. Rev.* 295 (2015) 125.
- [11] Q.Y. Li, Y. Quan, W. Wei, J. Li, H. Lu, R. Ni, X.J. Wang, *Polyhedron* 99 (2015) 1.
- [12] Y. Li, N. Wang, Y.J. Xiong, Q. Cheng, J.F. Fang, F.F. Zhu, Y. Long, S.T. Yue, *New J. Chem.* 39 (2015) 9872.
- [13] X. Wang, J. Zhao, Y. Zhao, H. Xu, X. Shen, D.R. Zhu, S. Jing, *Dalton Trans.* 44 (2014) 9281.
- [14] P.F. Shi, H.C. Hu, Z.Y. Zhang, G. Xiong, B. Zhao, *Chem. Commun.* 51 (2015) 3985.
- [15] T. Grancha, A. Acosta, J. Cano, J. Ferrando-Soria, B. Seoane, J. Gascon, J. Pasan, D. Armentano, E. Pardo, *Inorg. Chem.* 54 (2015) 10834.
- [16] R. Wang, X.Y. Dong, H. Xu, R.B. Pei, M.L. Ma, S.Q. Zang, H.W. Hou, T.C.W. Mak, *Chem. Commun.* 50 (2014) 9153.
- [17] Q. Tang, S. Liu, Y. Liu, D. He, J. Miao, X. Wang, Y. Ji, Z. Zheng, *Inorg. Chem.* 53 (2014) 289.
- [18] L. Liu, C. Huang, X. Xue, M. Li, H. Hou, Y. Fan, *Cryst. Growth Des.* 15 (2015) 4507.
- [19] B. Liu, Y.H. Jiang, Z.S. Li, L. Hou, Y.Y. Wang, *Inorg. Chem. Front.* 2 (2015) 550.
- [20] T. Grancha, J. Ferrando-Soria, H.C. Zhou, J. Gascon, B. Seoane, J. Pasan, O. Fabelo, M. Julve, E. Pardo, *Angew. Chem., Int. Ed.* 54 (2015) 6521.
- [21] T. Kajiwara, M. Fujii, M. Tsujimoto, K. Kobayashi, M. Higuchi, K. Tanaka, S. Kitagawa, *Angew. Chem., Int. Ed.* 55 (2016) 2697.
- [22] B.F. Abrahams, A.D. Dhama, B. Dyett, T.A. Hudson, H. Maynard-Casely, C.J. Kingsbury, L.J. McCormick, R. Robson, A.L. Sutton, K.F. White, *Dalton Trans.* 45 (2016) 1339.
- [23] R.S. Pillai, V. Benoit, A. Orsi, P.L. Llewellyn, P.A. Wright, G. Maurin, *J. Phys. Chem. C* 119 (2015) 23592.
- [24] R.A. Agarwal, S. Mukherjee, *Polyhedron* 106 (2016) 163.
- [25] L. Wen, X. Wang, H. Shi, K. Lv, C. Wang, *RSC Adv.* 6 (2016) 1388.
- [26] B. Gole, A. Kumar, P.S. Mukherjee, *Chem. Eur. J.* 20 (2014) 2276.

- [27] C. Zhang, Y. Yan, Q. Pan, L. Sun, H. He, Y. Liu, Z. Liang, J. Li, *Dalton Trans.* 44 (2015) 13340.
- [28] L. Li, J.Y. Zou, S.Y. You, Y. Hu, Q.R. Ji, K.H. Chen, J.Z. Cui, *Inorg. Chem. Commun.* 60 (2015) 111.
- [29] W.H. Huang, J.Z. Li, T. Liu, L.S. Gao, M. Jiang, Y.N. Zhang, Y.Y. Wang, *RSC Adv.* 5 (2015) 97127.
- [30] Y.L. Hou, H. Xu, R.R. Cheng, B. Zhao, *Chem. Commun.* 51 (2015) 6769.
- [31] Y.C. Ou, X. Gao, Y. Zhou, Y.C. Chen, L.F. Wang, J.Z. Wu, M.L. Tong, *Cryst. Growth Des.* 16 (2016) 946.
- [32] M.X. Zheng, X.J. Gao, C.L. Zhang, L. Qin, H.G. Zheng, *Dalton Trans.* 44 (2015) 4751.
- [33] J.Z. Qiu, Y.C. Chen, L.-F. Wang, Q.W. Li, M. Orendáč, M.L. Tong, *Inorg. Chem. Front.* 3 (2016) 150.
- [34] X.Q. Wu, M.L. Han, G.W. Xu, B. Liu, D.S. Li, J. Zhang, *Inorg. Chem. Commun.* 58 (2015) 60.
- [35] L. Zhang, L. Liu, C. Huang, X. Han, L. Guo, H. Xu, H. Hou, Y. Fan, *Cryst. Growth Des.* 15 (2015) 3426.
- [36] A. Bajpai, P. Chandrasekhar, S. Govardhan, R. Banerjee, J.N. Moorthy, *Chem. Eur. J.* 21 (2015) 2759.
- [37] Y. Fan, C.D. Si, C. Hou, X.Q. Yao, D.C. Hu, Y.X. Yang, J.C. Liu, *Polyhedron* 98 (2015) 64.
- [38] Y.S. Yue, Y. He, L. Zhou, F.J. Chen, Y. Xu, H.B. Du, X.Z. You, B. Chen, *J. Mater. Chem. A* 1 (2013) 4525.
- [39] L. Zhou, J. Zhang, Y.Z. Li, H.B. Du, *CrystEngComm* 15 (2013) 8989.
- [40] T. Wang, C. Zhang, Z. Ju, H. Zheng, *Dalton Trans.* 44 (2015) 6926.
- [41] S. Sen, S. Neogi, A. Aijaz, Q. Xu, P.K. Bharadwaj, *Dalton Trans.* 43 (2014) 6100.
- [42] R. Mishra, M. Ahmad, M.R. Tripathi, R.J. Butcher, *Polyhedron* 50 (2013) 169.
- [43] X. Hou, S.F. Tang, *RSC Adv.* 4 (2014) 34716.
- [44] P. Thuéry, B. Masci, J. Harrowfield, *Cryst. Growth Des.* 13 (2013) 3216.
- [45] J.J. Huang, W. Xu, Y.N. Wang, J.H. Xu, P. Zhang, J.Q. Xu, *J. Solid State Chem.* 226 (2015) 206.
- [46] Y.N. Wang, P. Zhang, J.H. Yu, J.Q. Xu, *Dalton Trans.* 44 (2015) 1655.
- [47] Y.N. Wang, J.H. Yu, J.Q. Xu, *ChemPlusChem* 80 (2015) 1732.
- [48] J.J. Huang, X. Zhang, Q.S. Huo, J.H. Yu, J.Q. Xu, *Inorg. Chem. Front.* 3 (2016) 406.
- [49] Y.N. Wang, W.C. Zhu, Q.S. Huo, J.H. Yu, J.Q. Xu, *Spectrochim. Acta A* 161 (2016) 138.
- [50] G.M. Sheldrick, *Acta Crystallogr., Sect. A: Found. Crystallogr.* 64 (2008) 112.
- [51] H.L. Jia, M.J. Jia, H. Ding, J.H. Yu, J. Jin, J.J. Zhao, J.Q. Xu, *CrystEngComm* 14 (2012) 8000.
- [52] J.J. Zhao, X. Zhang, Y.N. Wang, H.L. Jia, J.H. Yu, J.Q. Xu, *J. Solid State Chem.* 207 (2013) 152.
- [53] H.L. Jia, M.J. Jia, G. Zeng, J. Jin, J.H. Yu, J.Q. Xu, *CrystEngComm* 14 (2012) 6599.
- [54] Q. Hou, M.J. Jia, J.J. Zhao, J. Jin, J.H. Yu, J.Q. Xu, *Inorg. Chim. Acta* 384 (2012) 287.
- [55] G.X. Liu, K. Zhu, H.M. Xu, S. Nishihara, R.Y. Huang, X.M. Ren, *CrystEngComm* 12 (2012) 1175.
- [56] G.X. Liu, R.Y. Huang, L.F. Huang, X.J. Kong, X.M. Ren, *CrystEngComm* 11 (2009) 643.
- [57] X.M. Gao, D.S. Li, J.J. Wang, F. Fu, Y.P. Wu, H.M. Hu, J.W. Wang, *CrystEngComm* 10 (2008) 479.
- [58] G.P. Yang, R.T. Liu, C. Ren, L. Hou, Y.Y. Wang, Q.Z. Shi, *Inorg. Chim. Acta* 394 (2013) 58.